Influence of cyclic load on accumulated pullout displacement and pullout stiffness of geogrid reinforced soil structures

Kamer Charan[1] and Kenji Watanabe[2]

[1] Department of Civil Engineering, The University of Tokyo, 7-3-1, Bunkyo, Hongo, Tokyo, Japan. (Currently Penta Ocean Construction Co ltd, 1534-1 Yonkucho, Nasushiobara, Tochigi, Japan)
[2] Department of Civil Engineering, The University of Tokyo, 7-3-1, Bunkyo, Hongo, Tokyo, Japan.

ABSTRACT

The long girders in Japanese GRS-Integral bridges experience expansion and contraction due to the seasonal temperature variation. The geogrid in the GRS Integral bridge gets affected by these actions in a cyclic loading manner. Also, the designing of the GRS structures is mostly done based on the in-isolation stiffness (*E*) instead of the mobilized pullout stiffness (*J*) due to the lack of understanding which causes inaccurate performance prediction. Therefore, in this study, an experimental investigation has been conducted to understand this phenomenon. From this study, it is understood that in the in-isolation stage, cyclic loading did not lead to displacement accumulation. Meanwhile, there was a significant accumulation of pullout displacement under cyclic loading in the pullout stage. The soft geogrid exhibited higher accumulated displacements compared to the stiff geogrid. Also, under the cyclic loadings, the pullout stiffness (*J*) has shown degradation in contrast to the in-isolation stiffness (*E*).

Keywords: Geogrid; GRS integral bridge; Cyclic loading; Pullout stiffness; and Accumulated displacement

1 INTRODUCTION

In Japan, the GRS-Integral bridges are widely used, because of their superior performance in the event of an earthquake (Tatsuoka et al 2009). These GRS Integral bridges generally have a large span for the girder (maximum 60m) which generates a significant thermal expansion and contraction during seasonal changes, these expansion and contraction of the girder affect the geogrid reinforcement in the backfill soil in the cyclic loading manner. Also, the current practice of designing GRS structures is mainly based on the geogrid strength and the In-isolation stiffness (*E*) rather than the mobilized pullout stiffness (*J*) (Watanabe et al 2022, Kameri et al 2023). This practice is in use because the understanding of the pullout stiffness (*J*) is limited, this is due to it depending on several parameters such as In-isolation stiffness (*E*), Interface stiffness (*M*), aperture size, soil particle size etc.

Several studies have investigated the behaviour of geosynthetics under cyclic loading. Raju and Fannin (1998) examined the influence of confining stress, specimen properties, and cyclic loading frequency on pullout resistance and deformation behaviour. Nayeri and Fakharian (2009) studied the pullout behaviour of uniaxial geogrids under monotonic and cyclic loading. Moraci and Cardile (2009, 2012) investigated the effect of cyclic tensile loads on pullout resistance and deformative behaviour. Abdel-Rahman and Ibrahim (2011) explored the factors controlling soil-geogrid interface behaviour under cyclic loading. Koshy and Unnikrishnan (2016) examined the effect of cyclic loading amplitude and normal stress on geogrid pullout resistance. Cardile et al. (2019) evaluated the pullout behaviour of geogrids under cyclic loading conditions. Watanabe et al. (2022) considered seasonal changes and evaluated the effect of cyclic loading on the pullout stiffness.

To the best of the author's knowledge, the understanding of the characteristics of pullout stiffness (*J*) of geogrid subjected to cyclic loading is limited. Therefore, this paper aims to address this knowledge gap by conducting an experimental study.

1.1 Introduction to interface stiffness (*M*)

Interface stiffness (*M*) is a shear stiffness at the interface of geogrid and soil, which represents the interface conditions. Directly evaluating this interface stiffness (*M*) is difficult because of its non-linear behaviour and difficult to measure directly, therefore a mathematical model was developed (equations (1) to (3)) in the extended research to calculate the interface stiffness (*M*). This mathematical model requires data of in-isolation stiffness (*E*), pullout stiffness (*J*) and mobilized tensile force (*T(x)*) over the entire geogrid length for calculation of interface stiffness (*M*).

$$\alpha = \sqrt{\frac{E}{M}} \quad (1)$$

$$T(x) = P_0 \cdot \frac{[exp\{(2L - x)/\alpha\} - exp(x/\alpha)]}{[exp(2L/\alpha) - 1]} \quad (2)$$

$$J = \frac{P_0}{s_0} = \sqrt{M \cdot E} \cdot \frac{[exp(2L/\alpha) - 1]}{[exp(2L/\alpha) + 1]} \quad (3)$$

Where:

α – characteristic length (m)
T(x) – Tensile force at the x on the geogrid at the interface (kN/m)
P_0 – Applied pullout force (kN/m)
S_0 – Pullout displacement (m)
L – Geogrid length (m)
J – Pullout stiffness (kN/m/m)
E – In-isolation stiffness (kN/m)
M – Interface stiffness (mPa/m)

2 MATERIALS AND EXPERIMENTAL PROGRAM

Two types of geogrids were used for this study. Those geogrids are made of PVA (Poly Vinyl Alcohol) fibre and Nylon 66 (Table) also two types of soils (Table 2) were used. The main difference among the soil types used in this research is their mean diameter and shear stiffness of soil. The difference between the two geogrids is mainly their in-isolation stiffness (*E*).

Table 1. Details of the geogrids used.

Material	Geogrid-1	Geogrid-3
Parent material	PVA	Nylon 66
Aperture size (mm)	23 × 15	20 × 20
Width of rib (Long× Tran)	7 × 4	6 × 6
Aperture opening ratio (%)	51	49
Tensile strength (kN/m)	101	106
In-Isolation stiffness @ 5% strain (kN/m)	980	290

Table 2. Details of the soils used.

Soil	$\gamma_{d\text{-}max}$ g/cm^3	D_{50} mm	σ_c kPa	Young's modulus E_0 GPa	Young's modulus E_{50} GPa	Shear strength q_{max} MPa
Soil -1	1.806	6.0	20	0.73	0.100	0.670
Soil -2	1.542	0.18	60	0.12	0.028	0.255

The in-isolation experiments and pullout experiments were performed in this research. The schematic diagram of the pullout experiments is shown in Fig. 1. In the pullout test, the telltales were also used.

All the pullout experiments were conducted under a confining pressure of 60 kPa. All the experiments including in-isolation and pullout tests were conducted at a displacement rate of 1mm/min, to eliminate the displacement rate effect.

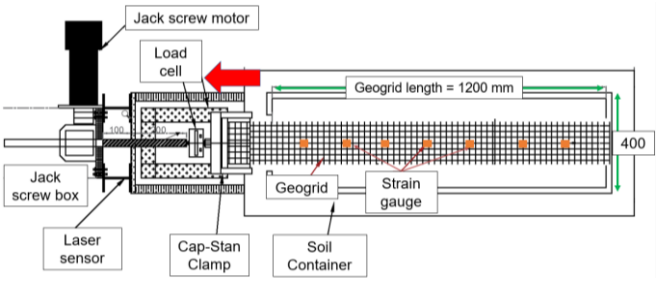

Fig. 1. Schematic diagram of Pullout apparatus

In this research, to measure the local strains of the geogrids at the interface of soil and geogrid the strain gauge method was developed (Kameri et al., 2023).

The cyclic loadings were applied starting at 1 kN/m and increased to the selected amplitude of force. The application of cyclic loadings continued until the accumulation of displacement became negligible. In this study, three force amplitudes were used: 5 kN/m, 10 kN/m, and 20 kN/m, for both experiments.

3 RESULTS AND DISCUSSION

3.1 Influence of cyclic load on the accumulated displacement

The in-isolation and the pullout tests were conducted on the geogrids under cyclic loading, to understand the influence of the cyclic loading. From these experimental results, it is understood that the tendency of accumulation of displacements is higher in the pullout stage (Fig. 2) compared to the in-isolation stage (Fig. 3).

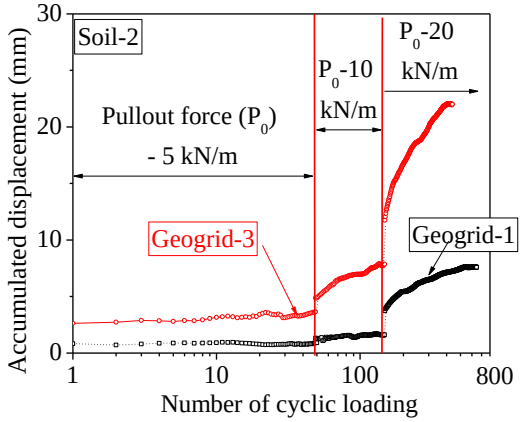

Fig. 2 Accumulated pullout displacement in pullout state, under cyclic loading

In the in-isolation state, the geogrid displacement becomes stable at the initial stage of cyclic loadings, however in the pullout state the gradual increase of pullout displacement seems to be increasing with the cyclic loading. This behaviour might have occurred because of the degradation of soil's contribution at the interface of soil and geogrid in the pullout test. Such as degradation of shear resistance and rearrangement of soil particles. This phenomenon is evident as the mobilized

local strains on the geogrid at the interface were increasing with cyclic loading (Fig. 5 and Fig. 6).

With this increase in the local strains, the frictional resistance at the interface of the geogrid and soil is likely to degrade. In addition to the frictional resistance the bearing resistance of transverse ribs also contributes to the pullout resistance, however, in this case, the bearing resistance may not be changing because the displacements at the interface are not high enough to degrade the bearing resistance as explained in the (Alagiyawanna et al., 2001).

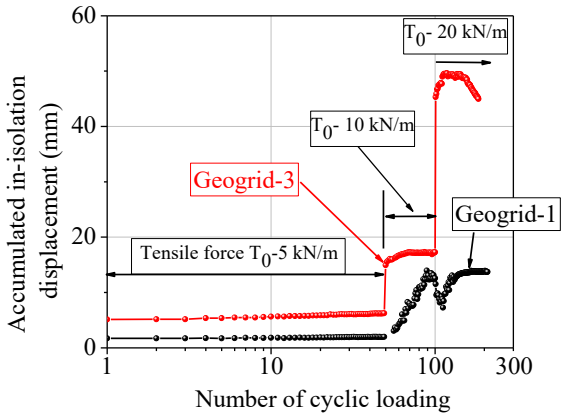

Fig. 3. Accumulated displacement of geogrid under in-isolation state for cyclic loading

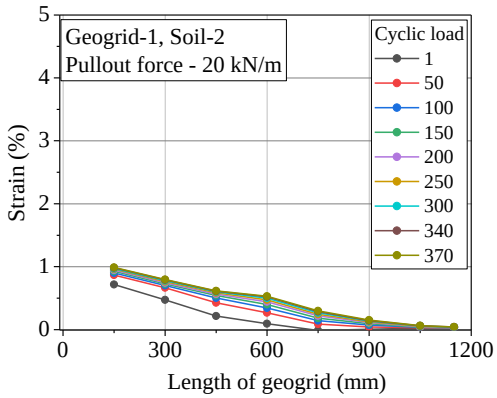

Fig. 4. Tensile strain distribution along the geogrid length under pullout force of 20 kN/m for Geogrid-3 under the cyclic loading

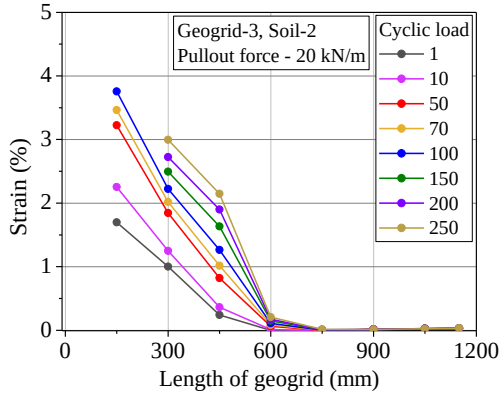

Fig. 5. Tensile strain distribution along the geogrid length under pullout force of 20 kN/m for Geogrid-3 under the cyclic loading

3.2 Influence of in-isolation stiffness under cyclic loading

As explained in the material section two types of geogrids were used in this study, the geogrids have similar geometrical characteristics, the difference among them is their in-isolation stiffness (E) which makes an ideal scenario to understand the influence of in-isolation stiffness. From the experimental study, it is understood that with the higher in-isolation stiffness (E) the accumulated displacements will be lower compared to the lower in-isolation stiffness (E) geogrid as shown in Fig. 2.

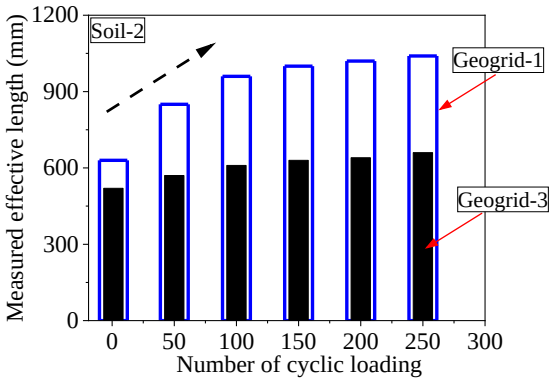

Fig. 6. Propagation of effective length (L_{eff}) of Geogrid-3 under cyclic loading at a pullout force amplitude of 20 kN/m

To explain the reason, it is required to evaluate the local strains at the interface as well as the effective length. The effective length is the length of geogrid at the interface which contributes to the pullout resistance. In this research, it is defined as part of geogrid, which has a mobilized tensile force more than or equal to 5% of the applied pullout force. The calculated effective length (L_{eff}) is shown in Fig. 6.

From these results, it is demonstrated that the stiff geogrid (Geogrid-1) exhibits a higher effective length (L_{eff}), which tends to increase with the rise in cyclic loading. This trend is observed because in the high stiff geogrid, the local strains at the interface are distributed to longer lengths (Fig. 4), and the increase in local strains with cyclic loadings remains minimal. In contrast, soft geogrid exhibits a shorter effective length and negligible increase with cyclic loading, resulting in a significant increase in local strains at the interface, as illustrated in Fig. 5. Therefore, from this trend it is understood that the higher rate of displacement accumulation under cyclic loadings for Geogrid-3 is attributed to not only the inherent in-isolation stiffness (E) of the geogrid but also due to the response of geogrid at the interface such as higher mobilization of local strains at the interface.

3.3 Influence of cyclic loading on pullout stiffness

In the pullout state of the geogrid under cyclic loading, pullout stiffness (J) experiences a gradual decrease with loading cycles, as depicted in Fig. 7. In contrast, in-isolation stiffness (E) does not exhibit a similar decrease under the application of cyclic loading, as illustrated in Fig. 8.

This observed phenomenon is attributed to the gradual degradation of interface stiffness (M) influenced by cyclic loading for a given pullout force amplitude.

Fig. 9 shows the degradation of interface stiffness (M) from the second cycle to the last cycle, indicating the weakening of the interface between soil and geogrid. Therefore, designing the GRS structures by relying only on the in-isolation stiffness (E) in practice leads to inaccurate performance prediction.

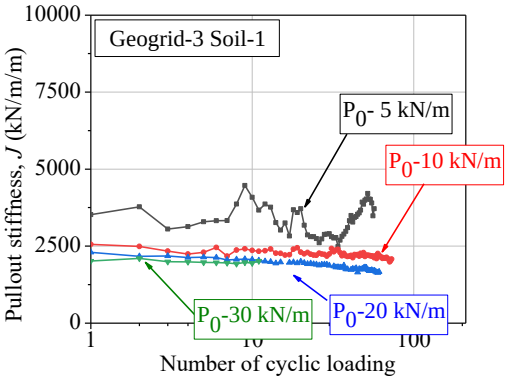

Fig. 7. Influence of cyclic loading on pullout stiffness.

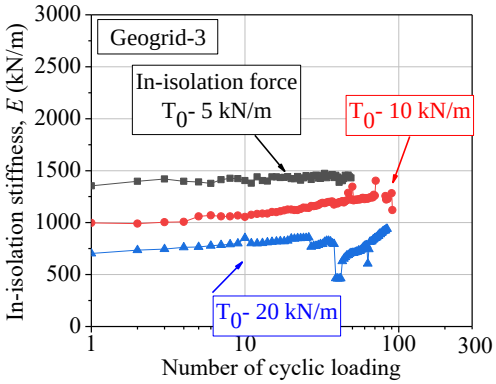

Fig. 8. Influence of cyclic loading on the in-isolation stiffness.

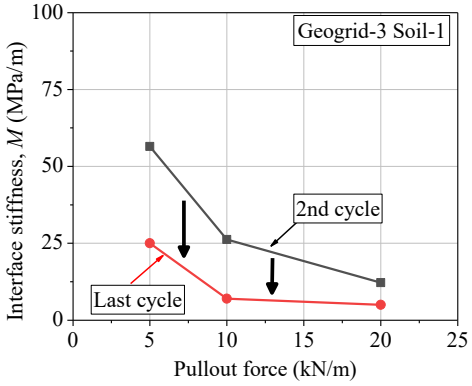

Fig. 9. Characteristics of interface stiffness under cyclic loading at three pullout amplitude forces of 5kN/m, 10 kN/m and 20 kN/m.

4 CONCLUSIONS

From large-scale pullout experiments conducted on the geogrids under the cyclic loading, several important conclusions were drawn regarding the behaviour of the geogrid at the interface those are:

Geogrid's behaviour under cyclic loading differs from those in the in-isolation stage. In the in-isolation stage, cyclic loading did not lead to displacement accumulation. Meanwhile, in the pullout stage, displacement accumulated under cyclic loading. This was due to the degradation of interlocking of soil and geogrid such as surface friction and bearing resistance of transverse ribs.

The soft geogrid (Geogrid-3) exhibited higher accumulated displacements at similar pullout force amplitudes compared to the stiff geogrid (Geogrid-1). This is due to not only the inherent properties of geogrids but also due to the characteristics of the interface.

The extended exposure to cyclic loading resulted in a noticeable reduction in the interface stiffness (M). This decrease directly impacted the pullout stiffness (J). The degradation of interface stiffness (M) represents the loss of frictional and transverse bearing resistance. Thus, an understanding of the characteristics of pullout stiffness (J) is required for the rational design of the GRS structures.

ACKNOWLEDGEMENTS

This research was carried out through a collaboration with Kuraray. The authors would like to Emirates Prof. Fumio Tatsuoka, Emirates Prof. Junichi Koseki and Asst Prof. Morimoto for their consideration and valuable comments.

REFERENCES

Abdel-Rahman, A. H., & Ibbrahim, M. A. M. (2011). Soil/geogrid behaviour subjected to cyclic loading. In Geo-Frontiers 2011: Advances in Geotechnical Engineering (pp. 3087-3096).

Alagiyawanna, A.M.N., Sugimoto, M., Sato, S., Toyota, H., (2001). Influence of longitudinal and transverse members on geogrid pullout behaviour during deformation, Geotextiles and Geomembranes.

Cardile, G., Pisano, M., & Moraci, N. (2019). The influence of a cyclic loading history on soil-geogrid interaction under pullout condition. Geotextiles and Geomembranes, 47(4), 552-565.

Kameri, C., & Watanabe, K. (2023). Characterization of pullout stiffness of geogrid considering the interaction with soil. Geosynthetics Engineering Journal, 38, 156-163.

Koshy, N., & Unnikrishnan, N. (2016). Geosynthetics under cyclic pullout and post-cyclic monotonic loading. International Journal of Geosynthetics and Ground Engineering, 2, 1-6.

Moraci, N., & Cardile, G. (2009). Influence of cyclic tensile loading on pullout resistance of geogrids embedded in a compacted granular soil. Geotextiles and geomembranes, 27(6), 475-487.

Moraci, N., & Cardile, G. (2012). Deformative behaviour of different geogrids embedded in a granular soil under monotonic and cyclic pullout loads. Geotextiles and Geomembranes, 32, 104-110.

Nayeri, A., & Fakharian, K. (2009). Study on pullout behavior of uniaxial HDPE geogrids under monotonic and cyclic loads.

Watanabe, K., Kojima, K., Kudo, A., (2022). Influence of cyclic load on pullout stiffness of geogrid embedded in well-graded gravel. Geosynth Int 29, 442–456.

Raju, D.M., Fannin, R.J., (1998). Load-strain-displacement response of geosynthetics in monotonic and cyclic pullout.

Tatsuoka, F., Hirakawa, D., Nojiri, M., Aizawa, H., Nishikiori, H., Soma, R., ... & Watanabe, K. (2009). A new type of integral bridge comprising geosynthetic-reinforced soil walls. Geosynthetics International, 16(4), 301-326.